Evaluation of Anticancer Activity of Lactobacillus-Synthesized Zinc Oxide Nanoparticles against MCF-7 Human Breast Cancer Cells

Anjana M.I., Abiyoga M., Rajalakshmy K. and Saravana Kumari P.*
Department of Microbiology, Rathnavel Subramaniam (RVS) College of Arts and Science, Coimbatore, Tamil Nadu, INDIA
*sarankumaribs@gmail.com

Abstract

This study explores the anticancer potential of zinc oxide nanoparticles (ZnONPs) synthesized using the cell-free supernatant of Lactobacillus *sp. The biosynthesis process utilized the Lactobacillus sp., culture supernatant as a biological reducing and capping agent, yielding stable ZnONPs. The synthesized ZnONPs were characterized comprehensively through UV-Vis spectroscopy, FTIR, XRD, SEM, TEM, EDX, Zeta potential and DLS analyses. UV-Vis spectra revealed a significant absorption peak at approximately 365 nm. Electron microscopy and XRD validated the spherical/cubic crystalline structure of ZnONPs, averaging 25-40 nm in size. Strong signals in EDAX spectrum confirmed ZnONPs formation. Zeta potential and DLS analysis showed biosynthesised ZnONPs stability and particle size.*

Morover, the anticancer activity was assessed against the human breast cancer cell line (MCF-7). Cell viability assays revealed a dose- and time-dependent cytotoxic effect of the ZnONPs. Morphological changes characteristic of apoptosis, cell shrinkage and nuclear fragmentation, were confirmed using acridine orange/ethidium bromide (AO/EB) staining. Flow cytometry demonstrated cell cycle arrest and apoptotic induction by the nanoparticles. ZnONPs also reduced the migratory potential of the MCF-7 cells in vitro. These findings highlight the eco-friendly synthesis of ZnONPs using Lactobacillus sp. *and their promising application in cancer nanomedicine as a novel, safe and effective therapeutic approach for breast cancer treatment.*

Keywords: Biosynthesis, Drug delivery, *Lactobacillus* spp., Anti-cancer activity, MCF-7 cancer cell line.

Introduction

Cancer remains one of the most significant global health challenges, characterized by the uncontrolled growth and spread of anomalous cells that can arise in virtually any tissue[10]. Numerous diseases with distinct biological behaviors and risk factors are the major causes of cancer. Further, the intricacy of cancer is inclined by various features including genetic modifications, environmental exposures and lifestyle choices smoking, diet and infections. Breast cancer is the most common malignancy in women leading to 6,70,000 deaths annually[41]. Women above 40 years are at greater risk and 13.1% of the women were diagnosed as positive. The conventional method of treating cancer cells is chemotherapy, but its application has been limited due to limitations like diagnosis during advanced stages, tumor resistance and adverse effects in patients[19].

Exceptional embattled activities and wide range of uses, metal nanoparticles have attracted much attention in recent decades. Zinc oxide nanoparticles (ZnONPs) have garnered significant research attention owing to their beneficial properties, which encompass stability under extreme environmental conditions, high photosensitivity, substantial excitation binding energy, cost-effectiveness, ease of fabrication, biocompatibility and environmental sustainability. Along with these uses, ZnONPs are widely used in the biomedical industry in fields such as drug delivery systems, anticancer therapies, antimicrobial treatments, antioxidant activities, anti-inflammatory responses and wound healing applications[26,34]. These nanoparticles are synthesized by chemical, physical, or biological means.

By biological methods, plant-mediated synthesis requires the extraction of bioactive chemicals from the plants. Compared to this cumbersome process, the bacteria possess a distinct advantage in the production of ZnONPs due to their ease of reproducibility at short period of time[5]. Over the past decade, there has been growing interest in using microbes such as bacteria, actinomycetes, fungi and yeast, to synthesize ZnONPs. These organisms function as small nano-factories, secreting enzymes, proteins, or biomolecules that selectively convert metal ions into their corresponding metal or metal oxide nanoparticles[28]. ZnONPs can be produced by a variety of microorganisms, although bacteria are preferred over other eukaryotic microorganisms due to their ease of handling and greater genetic manipulability[44].

Due to their non-pathogenic nature and the ability to produce a wide variety of enzymes harmless nature, the reproducible bacteria such as lactic acid bacteria (LAB) have attracted increased interest in the synthesis of nanoparticles mediated by bacteria. LAB is also widely found in a variety of food products and is recognized for its health-promoting qualities[27].

Lactobacillus, a genus of Gram-positive bacteria known for its probiotic properties, provides a green synthesis pathway

by reducing zinc salts into nanoparticles through its metabolites such as organic acids, enzymes and extracellular proteins. This eco-friendly approach aligns with green chemistry principles, reducing the need for toxic chemicals and harsh synthesis conditions[50]. ZnONPs derived from the genus Lactobacillus exhibit exceptional antimicrobial properties, primarily through the generation of reactive oxygen species (ROS) and disruption of microbial membranes[21]. These characteristics make them highly effective against both Gram-positive and Gram-negative bacteria, as well as fungi.

Zinc nanoparticles synthesized using *Lactobacillus sp.,* have gained prominence as a sustainable and biologically compatible alternative to chemically derived nanoparticles. Beyond their antimicrobial applications, Lactobacillus-synthesized ZnONPs have been explored in areas such as drug delivery, wound healing and UV protection due to their high biocompatibility, stability and non-toxic nature[36]. These nanoparticles structure-property relationships have been further clarified by advances in characterization using methods such as X-ray diffraction (XRD), Scanning electron microscopy (SEM) and Dynamic light scattering (DLS), opening the door to specific applications in industry and medicine[49].

Because it can biosynthesize zinc nanoparticles, Lactobacillus is a flexible bio-factory for the manufacture of nanomaterials. This method highlights the promise of nanoparticles for tackling issues in healthcare and environmental applications by producing them with increased biological activity while also lessening their negative effects on the environment[7]. Therefore, employing either cell-biomass or cell-free supernatant, some investigations have been carried out to ascertain the effectiveness of probiotic Lactobacillus in mediating the biogenesis of ZnONPs[21,35].

In this work, *Lactobacillus* sp., a type of lactic acid bacteria, was employed to synthesize biogenic ZnO nanoparticles. A variety of physicochemical characterizations were utilized to verify the formation of ZnO nanoparticles. The assessment of the cytotoxic effects, induction of apoptosis and cell cycle arrest of ZnONPs on MCF-7 cancer cells was performed to investigate the anticancer potential of ZnONPs.

Material and Methods

Zinc solution preparation: Zinc acetate ($ZnC_4H_6O_4$) was dissolved in deionized water to create a 1 M Zn^{2+} stock solution. The Zn^{2+} solution was filtered and subsequently added to the bacterial culture medium.

Biogenic synthesis of ZnONPs using *Lactobacillus* sp.: The biosynthesis of ZnO nanoparticles was performed with minor modification[24]. Lactobacillus bacteria were isolated from cow milk utilizing de Man, Rogosa and Sharpe (MRS) medium. A single colony of *Lactobacillus* sp., strain was then moved to sterile MRS broth and incubated at 37°C for 48 hours. The supernatant from the bacterial culture was obtained through centrifugation at 10,000 rpm for 10 minutes at a temperature of 4°C. The supernatant was subsequently combined with zinc acetate solution in 1:1 ratio and was allowed to incubate in the dark at 30°C for 24 hours. Following the incubation period, a noticeable color change signified the formation of ZnONPs.

Characterization of synthesized ZnO nanoparticles: To examine the optical, structural and microscopic properties of ZnONPs, several approaches have been used. The optical characteristics of ZnO nanoparticles were examined across wavelengths ranging from 200 to 600 nm through the application of UV Vis absorption spectroscopy (Hitachi U-2001- Tokyo, Japan). XRD was employed to assess the crystalline structure of the ZnO nanoparticles. The crystallization and phasing purity of ZnO nanoparticles were determined using X-ray diffraction (XRD Modelle – D8 Advance, BRUKER, Germany). An FT-IR (Fourier Transform Infrared) absorption spectrometer was employed to examine the functional groups present in the ZnONPs. FE-SEM (Carl- ZEISS Sigma 500 VP, Sigma, Osterode, Germany), EDAX (EDX, Bruker, Germany) and TEM (JEM-2100, JEOL, Tokyo, Japan) were employed to assess the purity of the elements.

The evaluation of the hydrodynamic diameter and zeta potential of the ZnONPs-Lb was conducted utilizing a Malvern Zetasizer Nanosystem (Worcestershire, UK). To begin with, the synthesized ZnONPs-Lb were placed in an aqueous solution and subsequently filtered using a 0.22 µm syringe-driven filter unit to guarantee uniform dispersion. A compact scattering spectrometer from the Malvern Zetasizer Nano series was then used to determine the size distribution of the ZnONPs-Lb using the DLS technique [1].

Anticancer activity of lactobacillus-mediated ZnONPs as a potential tool against human cancer cell line

Cell culture: Human breast cancer cells (MCF-7) were procured from the National Center for Cell Sciences (NCCS), Pune, India. These cells were cultured in Dulbecco's Modified Eagle Medium (DMEM), which was enriched with several essential components including L-glutamine, balanced salt solution (BSS), sodium carbonate (Na_2CO_3), non-essential amino acids, sodium pyruvate, glucose, HEPES buffer and fetal bovine serum. The medium was meticulously prepared to provide an optimal environment for cell growth and maintenance. Additionally, penicillin and streptomycin were incorporated at a concentration of 100 IU/100 µg per milliliter. The cells were incubated at 37°C in a humidified, CO_2-enriched atmosphere to ensure optimal growth conditions.

Evaluation of cytotoxicity: To determine the inhibitory concentration (IC_{50}) value, an MTT assay was conducted. MCF-7 breast cancer cells were seeded in a 96-well plate at a density of 1×10^4 cells per well and were allowed to grow for 48 hours until reaching approximately 80% confluence.

The existing medium was replaced with a fresh medium containing dilutions of ZnONPs-Lb. The cells were incubated for an additional 48 hours. Following this, the medium was discarded and 100 µl of MTT solution was added to each well with incubation at 37 °C for 4 hours. After removing the supernatant, 50 µl of DMSO was added to each well to dissolve the formazan crystals, followed by a 10-minute incubation. Optical density (OD) was measured at 620 nm using a Thermo Multiskan EX ELISA plate reader (USA). The OD values were then used to calculate cell viability percentages using the appropriate formula:

% of viability = OD value of experimental sample / OD value of experimental control × 100

Morphological Study: The MCF-7 cells were grown at a density of 1×10^5 cells per coverslip. The samples were subjected to ZnONPs-Lb treatment at different concentrations (10, 25 and 50 µg/ml) for 24 hours. Subsequently, the cells underwent fixation with a solution of ethanol and acetic acid in a 3:1 volume ratio. The coverslips were meticulously positioned on glass slides to facilitate the morphometric analysis. Images were captured of three monolayers within each experimental group. Using Nikon's bright field inverted light microscopy at a 10X magnification, the morphological changes of the cells were examined.

Fluorescence microscopic analysis of apoptotic cell death: A suspension of cells on microscope coverslips was mixed with a dye mixture of acridine orange (AO) and ethidium bromide (EtBr) diluted in 1 µl of distilled water. MCF-7 cancer cells were treated with different concentrations of ZnONPs-Lb. The cells were collected, rinsed with phosphate-buffered saline (PBS, pH 7.2) and stained using the AO/EtBr dye mixture. After 2-minute incubation, the cells were washed twice with PBS and were examined under a fluorescence microscope (Nikon Eclipse, Inc., Japan) at a magnification of 400X, utilizing a 580 nm excitation filter.

Cells were placed on glass coverslips in six-well plates and subjected to various concentrations of ZnONPs-Lb for 24 hours. The cells were treated with 0.2% Triton X-100 (50 µL) for 10 minutes at room temperature to permeabilize. 10 µl of DAPI stain and a coverslip were positioned over the cells to guarantee consistent staining. The cells were subsequently examined with the Nikon Eclipse fluorescence microscope.

Cell cycle analysis: Different concentrations (10 µg/ml, 25 µg/ml, 50 µg/ml) of the ZnONPs- Lb were applied to the chosen MCF-7 cell lines (2×10^5 cells/10 cm dishes) for 24 hours each. The cells underwent harvesting through centrifugation, followed by washing with ice-cold PBS and were subsequently re-suspended in ice-cold 70% ethanol for overnight. The cells were treated with 10µg/ml of RNase at 37°C, followed by centrifugation and staining with 40µg/ml of propidium iodide (PI) for 30 minutes. The DNA content was then measured by flow cytometry on a BD FACS Verse, USA.

Apoptotic protein expression analysis: The impact of ZnONPs-Lb on the expression of apoptotic and anti-apoptotic proteins in treated and untreated cells was investigated using Western blotting. MCF-7 cells (1.5×10^6) were cultured in 100 mm dishes and subjected to different concentrations of ZnONPs-Lb for 24 hours. After the treatment, the medium was discarded and the cells underwent several washes with phosphate-buffered saline (PBS). The cells were subsequently lysed with 0.1 ml of lysis buffer per plate for about 20 minutes, followed by centrifugation to obtain the supernatant, which functioned as the protein extract. Equal quantities of protein from each sample were subjected to separation on a 12% SDS-polyacrylamide gel through electrophoresis and then transferred to a nitrocellulose membrane.

The membranes were blocked with a solution of 10% skimmed milk in water for 1 hour, followed by washing with PBS that included 0.1% of Tween-20. Specific primary antibodies targeting p53, cytochrome C, Bcl-2 and β-actin were introduced at a dilution of 1:1000 and the mixture was incubated overnight at 4°C. Following the removal of the primary antibodies through washing, secondary antibodies were introduced and were allowed to incubate at room temperature for 1 hour. To determine the expression levels, the protein bands were visualized.

Gene expression studies by semi-quantitative reverse Transcriptase -Polymerase Chain Reaction (qRT-PCR) in breast cancer cells: A chemical treatment of MCF-7 human breast cancer cells was applied and an untreated control group was also created. Following a 24-hour treatment period, the medium was completely removed from the flask. Isolation of total RNA was performed using TriZol reagent and subsequently, reverse transcription of the RNA was conducted. The cDNA was obtained using the cDNA synthesis kit and then amplified according to the specified guidelines.

Apoptotic gene RT-PCR was performed using random primer pairs (forward and reverse 0.5 µL + 0.5 µL) in 20 µl reaction mixture. The 10X reaction buffer with 1.0 µl, cDNA as template (2 µL), 10 µl of master mix (25 mM/l MgCl2, 10 mM/l dNTPs, 2.5 U Taq polymerase) and the remaining volume being nuclease-free distilled water (7 µl) were taken.

For a total of 32 cycles of amplification, the primer was annealed at 55ºC for 40 seconds, denatured at 94ºC for 1 minute and then extended at 72ºC or 1 minute. The last extension was conducted at 72ºC for 10 minutes. The quantification of PCR products was performed through agarose gel electrophoresis. Image J software was used for data analysis and densitometry analysis was used to schematically portray the intensity values.

Statistical analysis: All data were examined by Analysis of Variance. Data were presented as mean standard deviation. Statistical investigation was performed using Graph Pad 5.0 (Graph Pad Software, Inc.). $P < 0.05$ indicates a statistically significant difference value.

Results and Discussion

Synthesis of lactobacillus-mediated ZnONPs Characterization: The characterization of ZnONPs-Lb was conducted using a range of techniques including UV-vis FTIR, XRD, SEM, TEM EDAX, Zeta potential and DLS analysis. The process included the bio-reduction of zinc acetate using a cell-free supernatant derived from the *Lactobacillus* sp.

UV–Visible Spectroscopy: A peak at approximately 365 nm was observed during the analysis of ZnONPs-Lb using a UV-vis spectrophotometer. The symmetrical structure of the band suggests that the particles are evenly distributed, providing evidence for their existence and stability (Fig. 1). The absorption peak shifted towards a shorter wavelength when compared to bulk ZnO, which has an absorption maximum at 379 nm[38]. The absorption spectrum of ZnO nanoparticles was observed between 330 nm and 390 nm[45].

FTIR studies: The Fourier-transform infrared (FTIR) transmittance spectra of ZnONPs-Lb provided insights into the functional groups and molecular interactions associated with their synthesis. The spectra depicted in fig. 2 reveal distinct bands ranging from 500 to 4000 cm^{-1}, which correspond to various chemical bonds and vibrational modes present in the nanoparticles. Prominent peaks were observed at 2002.11, 1639.49, 1355.96, 1035.77, 866.04, 829.39 and 690.52 cm^{-1}. The peak at 2002.11 cm^{-1} is indicative of C≡C or C≡N stretching vibrations, suggesting the presence of alkyne or nitrile groups, likely originating from the bacterial metabolites involved in nanoparticle synthesis[17,37]. The peak at 1639.49 cm^{-1} is attributed to C=O stretching vibrations, characteristic of amides or carboxyl groups, which are typically associated with proteins or organic acids that act as capping or stabilizing agents[46].

The peak at 1355.96 cm^{-1} corresponds to C-H bending vibrations, while the band at 1035.77 cm^{-1} is linked to C-O stretching, indicative of alcohol, ester, or ether groups[31]. Peaks at lower wave numbers, such as 866.04 and 829.39 cm^{-1}, are commonly associated with bending vibrations of out-of-plane C-H vibrations. Finally, the peak at 690.52 cm^{-1} represents Zn-O stretching vibrations, confirming the presence of ZnO nanoparticles[22,51]. These findings suggest that bacterial metabolites play a significant role in the reduction, stabilization and functional stabilization of the ZnONPs. The presence of organic functional groups highlights the potential biological origin and biocompatibility of the synthesized nanoparticles. Additionally, the distinct Zn-O vibrational peak further confirms the successful synthesis of ZnONPs using bacterial methods.

X-ray diffraction studies: The X-ray diffraction (XRD) analysis of ZnONPs confirmed their phase and crystalline structure, revealing a distinct diffraction pattern characteristic of a hexagonal wurtzite structure. Prominent peaks were observed at specific 2θ values corresponding to the crystallographic planes (hkl): (100), (002), (101), (102), (110), (103), (200), (112), (201), (004) and (202) (Fig. 3). These findings matched well with the reference data from the Joint Committee on Powder Diffraction Standards (JCPDS card No. 79–2205.), indicating high crystallinity and purity in the biosynthesized ZnONPs. Similarly, diffraction patterns were observed in ZnONPs synthesized using microbial methods, emphasizing the role of biosurfactants in enhancing nanoparticle stability and uniformity[3,22].

SEM Analysis: The SEM study of ZnONPs-Lb demonstrated primarily spherical nanoparticles measuring between 35 and 40 nm, as illustrated in fig. 4. The significant agglomeration found is characteristic of biosynthesised ZnO nanoparticles, likely due to their elevated surface energy and interparticle interactions. Recent research corroborates the synthesis of spherical ZnONPs via microbial processes, highlighting their restricted size distribution and propensity for agglomeration[40]. Previous studies have consistently reported that the biosynthesis of nanoparticles has resulted in spherical-shaped ZnONPs with uniform distribution[12]. Earlier research studies have explored the influence of surface morphology on the synergistic activity of ZnO[16]. The SEM analysis confirms the spherical morphology of the ZnO nanoparticles, indicating their characteristic shape as smooth edges, consistent with earlier findings[9,13].

TEM Analysis: Lactobacillus-mediated ZnONPs were examined for size and surface structure using Transmission Electron Microscopy (TEM), as illustrated in fig. 5. ZnONPs-Lb ranged in size from 28.3 nm to 48.0 nm according to TEM data. Fig. 5 shows that the NPs were spherical, evenly distributed and coated with probiotic molecules' bioactive components, which served as stabilising agents. The ZnONPs-Lb were successfully synthesised as a stabilizing agent, as seen by the grey colour layer around the ZnONPs-Lb in the TEM image. The reduction of Zinc ions was attributed to these bioactive components.

The capping of stabilising agents inhibits the agglomeration of ZnONPs. To verify that the nanoparticles were spherical, the scientists used high-resolution transmission electron microscopy (HR-TEM). Smilarly, the use of *Myristica fragrans* aqueous fruit extracts in the ecologically friendly manufacture of zinc oxide (ZnO) nanoparticles produced morphologies ranging from spherical to hexagonal[11]. The results were consistent with those of earlier research[32].

Energy Dispersive X-ray Analysis (EDX) Spectrum of ZnONPs: A study was conducted to determine the identification and quantification of elements in the ZnONPs.

This analysis relied on energy-dispersive X-ray spectroscopy, which detects the specific X-ray energies emitted by these elements. Based on the analysis, it was found that the ZnONPs contained zinc (Zn) and oxygen (O) atoms, as shown in fig. 6.

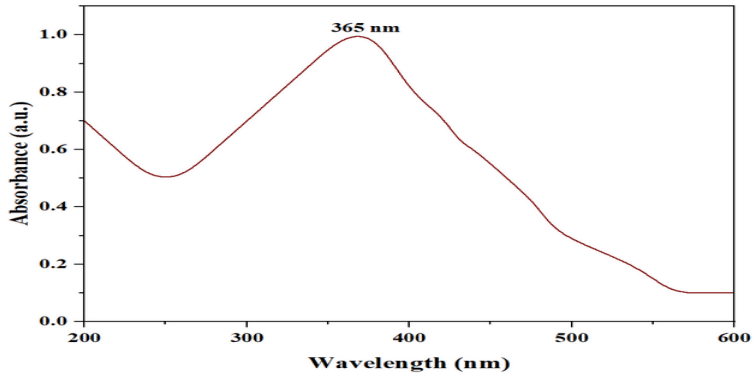

Figure 1: UV-visible spectrum of lactobacillus mediated ZnONPs

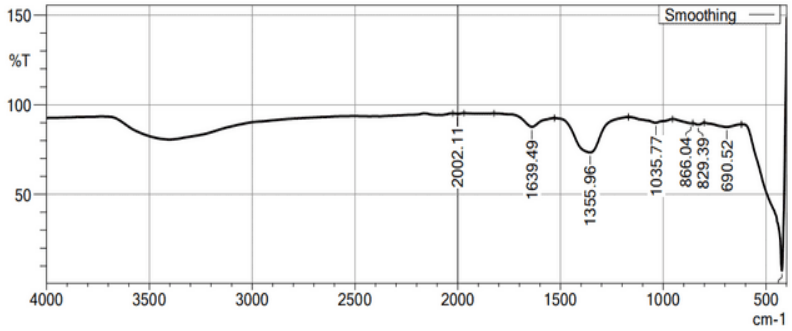

Figure 2: Fourier transform infrared spectroscopy analysis of lactobacillus mediated ZnONPs

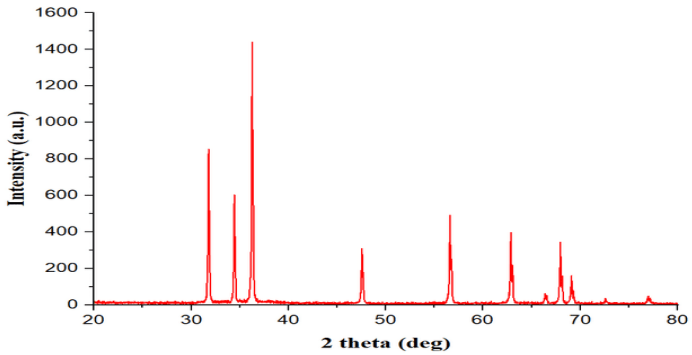

Figure 3: XRD analysis of lactobacillus mediated ZnO nanoparticles

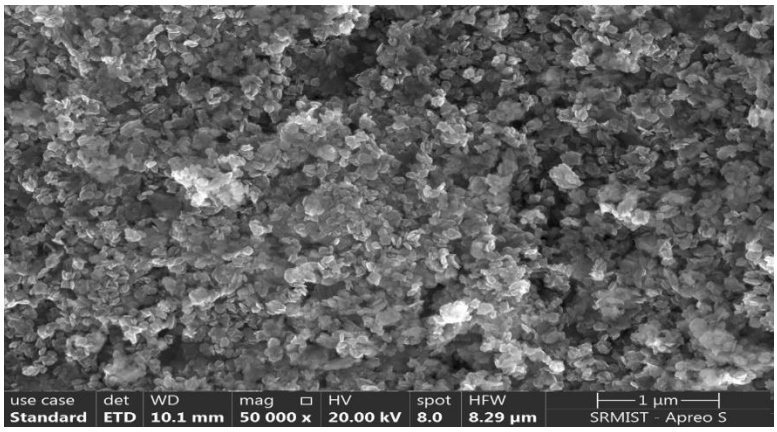

Figure 4: Scanning electron microscopy of lactobacillus mediated ZnONPs

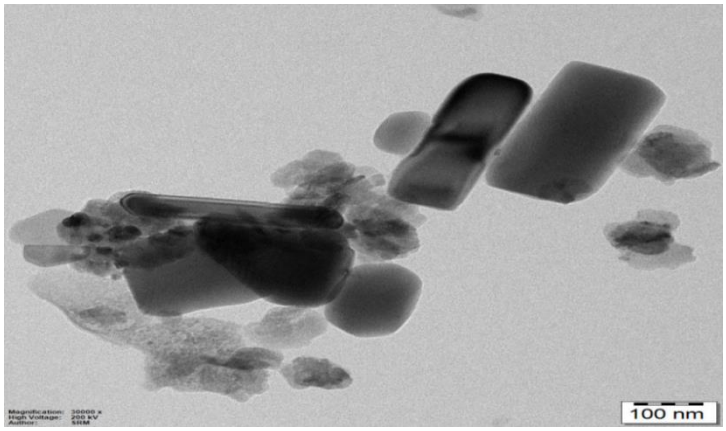

Figure 5: Scanning electron microscopy of lactobacillus mediated ZnONPs

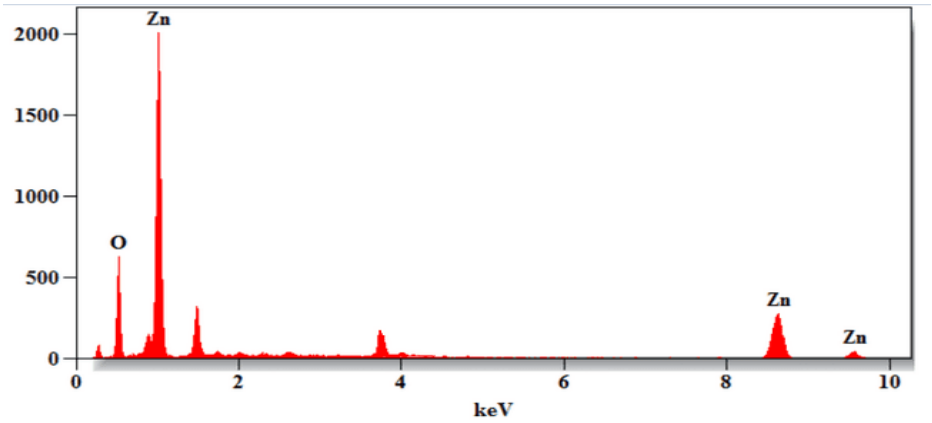

Figure 6: Energy dispersive X-ray analysis of lactobacillus mediated ZnONPs

These findings align with a previously published study that examined the composition of biosynthesized ZnONPs and found correlations between O and Zn composition[8,47,52].

Zeta potential of lactobacillus mediated ZnO nanoparticles: One of the most important factors in determining the stability of the produced nanoparticle is the suspension's zeta potential, which indicates the net electrostatic potential of all suspended particles. Strong electrostatic repulsive forces between the biosynthesised ZnONPs prevent agglomeration and their high positive potential value of 11.7 mv (Fig. 7) suggests that they were extremely stable. The electrostatic force of repulsion prevents strong negative or positive Zeta potential nanoparticles from aggregating whereas low Zeta potential particles tend to focus[35].

It is generally considered that the zeta potential values (+30 mV to −30 mV) result in good nanoparticle stability[23,35]. Our result is equivalent to the zeta potential of zinc nanoparticles made by *Pseudomonas hibiscicola*, which showed 24.64 mV[33]. Because of electrostatic attraction, positively charged nanoparticles adhere better to the surface of negatively charged cell membranes, allowing ZnONPs to enter cells and increase their toxicity towards microorganisms and nucleic acids[2].

Particle size and distribution (DLS) of the ZnONPs: One potential scattering method for analysing the size distribution and average particle size of NPs is dynamic light scattering (DLS). The Z-average size of the ZnONPs-Lb was 637.4 nm and their polydispersity index (PDI) was 0.382. Fig. 8 shows the DLS distribution histogram. The International Organisation for Standardisation (ISO) indicates that PDI values exceeding 0.7 suggest a broad distribution of the samples whereas PDI values below 0.5 indicate a higher degree of monodispersity. To compare the thickness of nanoparticles with the actual size of metal nanoparticles, DLS is a device that is typically used to measure the particle size of disperse solutions[39].

Exploring the anticancer potential of lactobacillus mediated ZnONPs against MCF-7 cells

MTT assay: Evaluation of the potential harm caused by ZnONPs (up to 100µg/ml) was done for 24 hours by MTT assay. Based on this experiment, it is evident that the ZnONPs-Lb had a significant impact on cell proliferation, with the inhibition being directly proportional to the dosage. The findings including the IC_{50} value, are displayed in table 1.

Fig. 9 demonstrates the significant impact of ZnONPs on reducing the growth of breast cancer cells. The IC_{50} values were found to be 30 µg/ml in breast cancer cells. By contrast, the standard cisplatin (standard) exhibited IC_{50} values of 16 µg/ml in breast cancer cells. ZnONPs revealed remarkable

efficacy against specific cancer cells when compared to conventional treatment methods.This finding has been supported by multiple studies[25,29,42].

It was observed that the cell line's viability decreased as the concentration of ZnONPs and standard drugs increased, which aligns with the findings[43]. There is a growing interest in the use of microbe-mediated ZnONPs as a potential anticancer therapy due to their low toxicity, surpassing chemically synthesized ZnONPs[14]. Previous research found that the MTT test, which utilized biosynthesized ZnONPs from *Lactobacillus* sp. extract, demonstrated phenomenal biocompatibility and showed a potential toxic effect of 54.16 µg ml^{-1} in the human colon cancer (HT-29) cell line[38].

Table 1
Cytotoxic activity of ZnONPs-Lb (concentrations in µg/ml)

Complex	MCF-7 cells (IC_{50})
ZnONPs-Lb	30 ±1.2
Cisplatin	16 ±0.8

IC_{50} – Values of respective Compounds (at 24 hrs)
Standard Used: Cisplatin

Morphological Analysis: The MCF-7 cancer cells were exposed to the IC_{50} concentration of ZnONPs-Lb for 24 hours, demonstrating a significant alteration in their morphology, as shown in fig. 10. There was a noticeable change in the appearance of the treated cells, which varied depending on the dosage. As the concentrations of ZnONPs-Lb increased, there was a corresponding increase in cytotoxicity. The extract caused cellular shrinkage, membrane blebbing, reorganization and a decrease in the total number of viable cells. These findings strongly indicated that the ZnONPs-Lb triggered apoptosis in MCF-7 cancer cells as shown in fig. 10 b, c and d. On the other hand, the untreated control cells exhibited no negative impacts (Fig. 10a).

The biosynthesized ZnONPs have the potential to disrupt cellular membranes, create vacuoles and alter the metabolism of cancer cells, thereby activating the apoptosis pathway and effectively eliminating cancer cells. Along with alterations in cellular and nuclear morphology, the presence of ZnONPs demonstrates effectiveness against the proliferation of HepG2 and MCF-7 cancer cells in a dose-dependent manner[48].

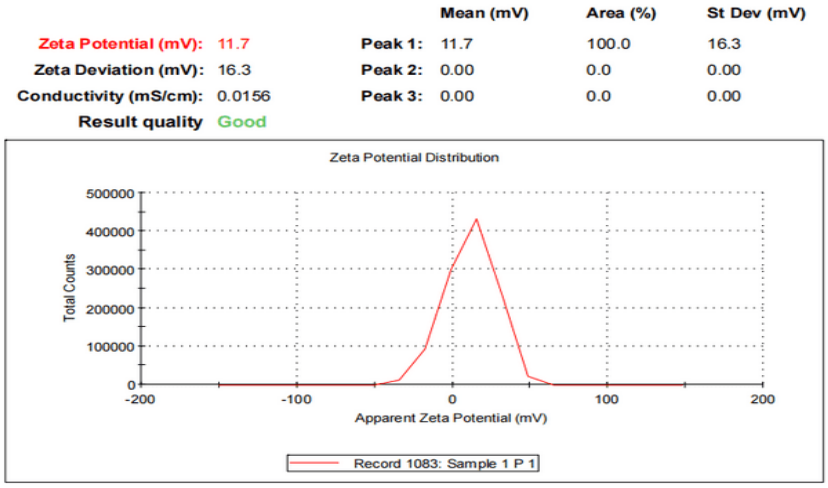

Figure 7: Zeta potential analysis of lactobacillus mediated ZnONPs

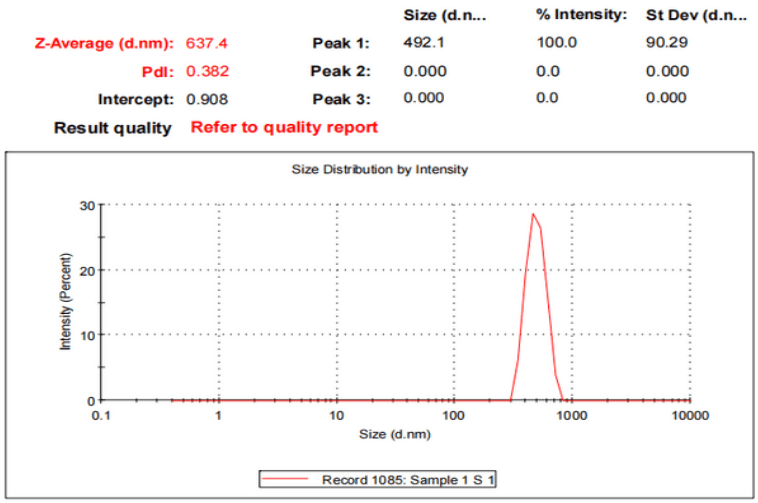

Figure 8: DLS analysis of lactobacillus mediated ZnO nanoparticles.

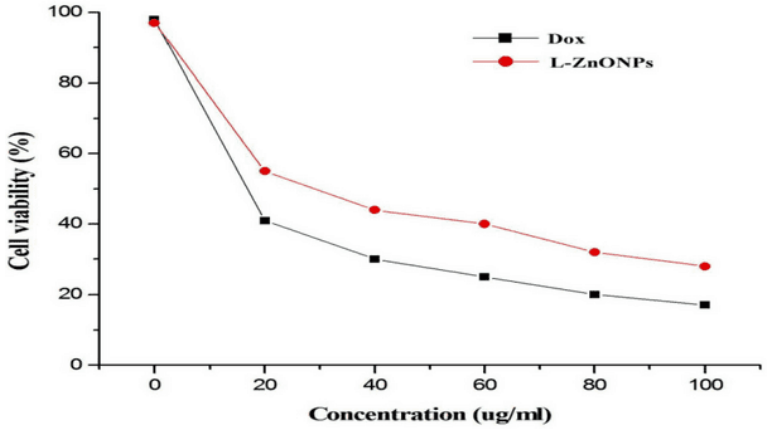

Figure 9: MTT analysis of lactobacillus-mediated ZnONPs on MCF-7 breast cancer cells

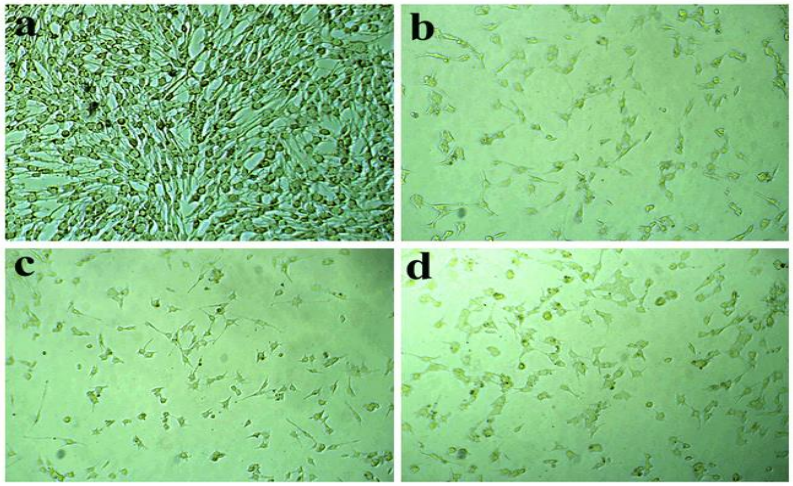

Figure 10: Morphological analysis of lactobacillus-mediated ZnONPs -treated MCF-7 cells for 24 hrs (a) Control (b)10 µg/ml (c) 25 µg/ml (d) 50 µg/ml

Fluorescence microscopic analysis of AO/EtBr and DAPI staining for nuclear fragmentation: The apoptogenic effects of ZnONPs-Lb were studied on selected cancer cells using fluorescence microscopy. Based on the observations, it was found that live cells emitted a vibrant green fluorescence, whereas dead cells emitted a distinct acridine orange fluorescence. Fig. 11a shows a unique abundance of viable cells in the untreated control cells. On the other hand, the MCF-7 cells treated with ZnONPs-Lb indicated an increased presence of cells undergoing apoptosis and the formation of apoptotic bodies. These were distinguishable by their unique characteristics, including nuclear shrinkage, nuclear damage and the development of blebs, which appeared as bodies emitting an orange/red coloration (Fig. 11b, c and d). It appears that the treatment caused apoptotic changes in MCF-7 cells, resulting in noticeable alterations that suggest apoptosis when examined.

Further, we evaluated the effectiveness of ZnONPs-Lb through DAPI staining. Fig. 12 provides a visual representation of the fluorescence microscopic images of the cells that have been stained with DAPI. It is worth mentioning that the cells treated with ZnONPs-Lb exhibited distinct characteristics. In MCF-7 cells, bright spots were observed, indicating the presence of clumped chromatins and fragmented nuclei (Fig. 12b, c and d for MCF-7 cells). On the other hand, fig. 12a does not exhibit any significant alterations in the cells. From the fluorescence microscopic analysis, it is evident that the ZnONPs showed great promise as a therapeutic agent in the treatment of cancer.

The study's results revealed a noteworthy suppression of growth in the MCF-7 cancer cell lines due to the ZnONPs-Lb. These findings align with previous research exploring the impact of nanoparticles on cell death in various cell types. The researchers investigated the process of apoptosis in human cervical cancer cells (HeLa cells) by utilizing copper oxide nanoparticles synthesized through green methods. These nanoparticles were found to effectively induce apoptosis in HeLa cells by promoting oxidative stress, causing mitochondrial dysfunction and altering the expression of key apoptosis-related proteins[29].

Effect of lactobacillus-mediated ZnO nanoparticles on cell cycle arrest by flow cytometry.: ZnONPs-Lb caused S phase transition arrest in the cells, according to the cell cycle analysis of the PI-stained cells. Fig. 13 shows that the ZnONPs-Lb suppressed the cell cycle at various stages. The

untreated control exhibited an increase in the number of cells during the G0-G1, S and G2/M phases. The proportion of cells in the G0/G1-phase showed a notable increase following treatment with the ZnONPs-Lb. Furthermore, the distribution of the DNA replication phase was diminished in relation to the treatment with the ZnONPs-Lb when contrasted with the control.

Fig. 13 showed that the ZnONPs's proliferative activity could be primarily attributed to its ability to induce cell cycle phase activation from arrest, primarily in the DNA duplication phase. According to Zhang et al[53], the G2/M phase arrest of the cell cycle can reduce growth and can trigger death by preventing damaged chromosomes from separation during mitosis. An earlier study discovered that UBQLN4 overexpression raised the percentage of GES-1 cells in the G2/M phase in comparison to the control cells.

This finding raises the possibility that the apoptotic program was initiated by a block in the G2/M transition[15]. It has been previously investigated that the ability of sitosterol-fabricated chitosan nanocomplexes to induce cell cycle arrest is the main factor responsible for their cell-inhibiting properties[18].

Western blot analysis: A wide range of apoptotic properties were measured using a western blot analysis in order to identify the mechanism of apoptosis triggered by the lactobacillus-mediated ZnONPs in the MCF-7 cells (Fig. 14). Notably, there was an increase in the expression of p53 and cytochrome c, which are apoptotic proteins, while a decrease was observed in Bcl-2, an anti-apoptotic protein. Interestingly, our results align with the mechanism whereby the depletion or inhibition of anti-apoptotic proteins triggers mitotic distress, DNA-damaging responses and ultimately, cell apoptosis.

By inhibiting the anti-apoptotic expression, the reduced level of Bcl-2 showed that chitosan nanocomplexes made with sitosterol effectively promoted the natural apoptotic activity[18].

A previous report established that apoptotic protein is crucial in counteracting the anti-apoptotic function of Bcl-2. In the mitochondrial-mediated natural apoptotic pathway, the overexpression of Bcl-2 inhibits caspase initiation and suppresses cytochrome c discharge from the mitochondria to the cytoplasm[53].

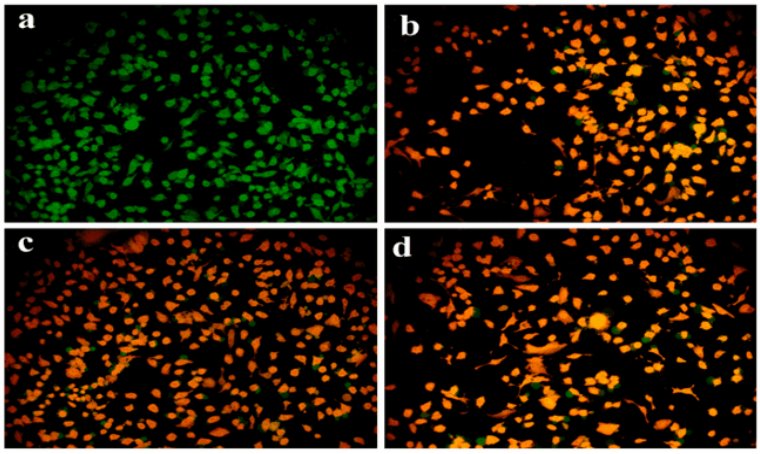

Figure 11:AO/EtBr staining assay of lactobacillus-mediated ZnO nanoparticles - treated MCF-7 cells (a) Control (b) 10 µg/ml (c) 25 µg/ml (d) 50 µg/ml

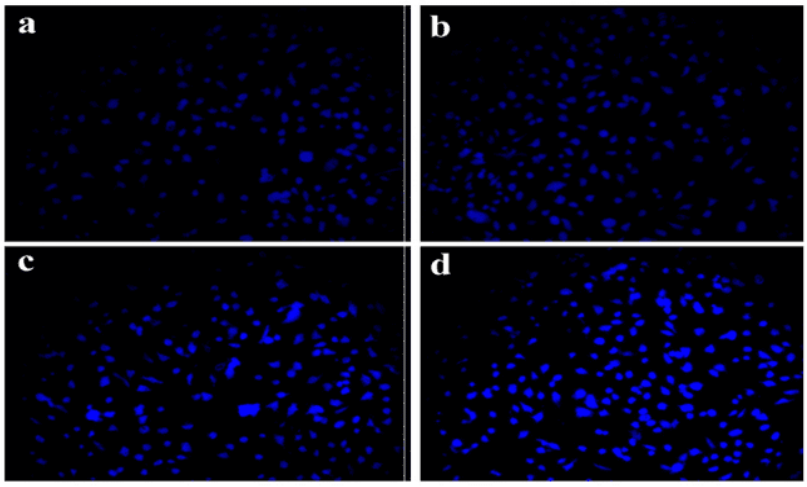

Figure 12: DAPI staining assay of lactobacillus-mediated ZnO nanoparticles - treated MCF-7 cells (a) Control (b) 10 µg/ml (c) 25 µg/ml (d) 50 µg/ml

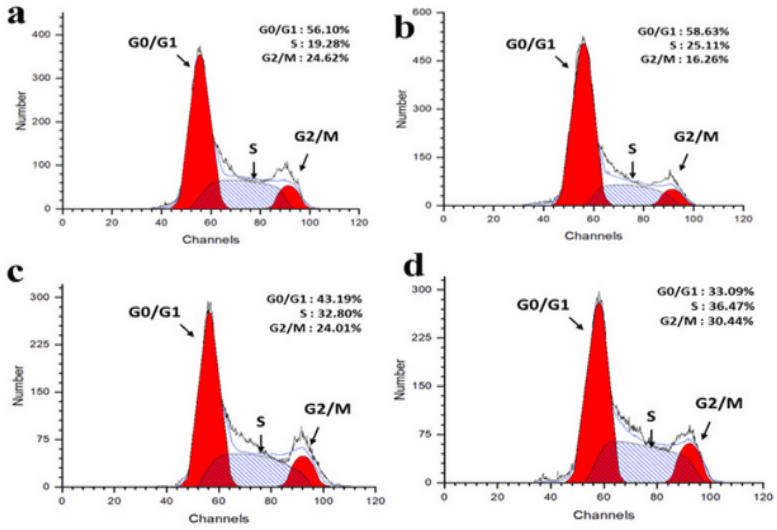

Figure 13: Induction of cell-cycle arrest through lactobacillus-mediated ZnO nanoparticles - treated MCF-7 cells (a) Control (b) 10 µg/ml (c) 25 µg/ml (d) 50 µg/ml

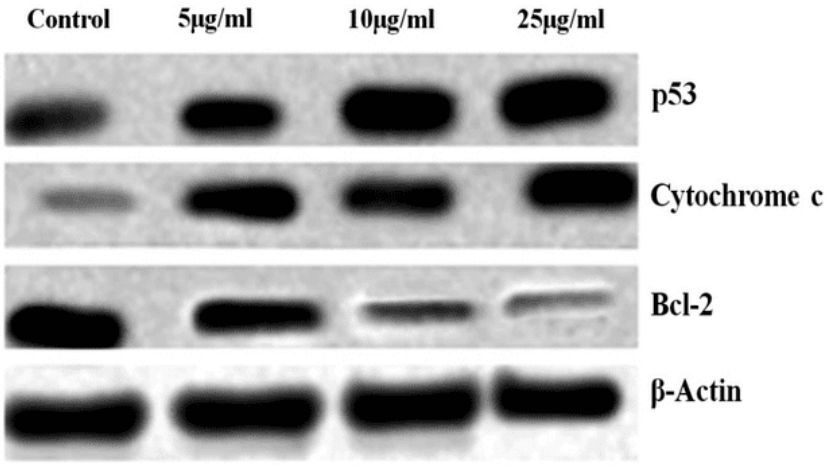

Figure 14: Expression of apoptotic and anti-apoptotic proteins by western blot analysis in MCF-7 cells treated with lactobacillus-mediated ZnO nanoparticles.

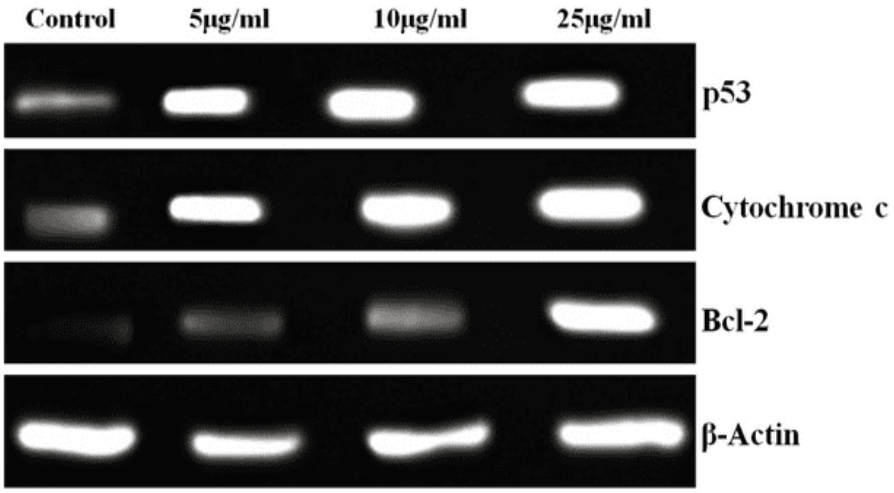

Figure 15: Effect of lactobacillus-mediated ZnO nanoparticles on the gene expression of apoptosis related genes

Semi-quantitative RT-PCR analysis for apoptotic gene expression: In this study, cancer cells exposed to varying concentrations of ZnONPs-Lb over 48 hours were used to analyse the expression of apoptotic genes using semi-

quantitative RT-PCR. The expression profiles of p53, cytochrome c, Bcl-2 and β-actin genes were checked and the results showed that ZnONPs-Lb -treated cancer cells had much higher levels of these genes than control, unexposed cells (Fig. 15). As compared to the corresponding controls with varying concentration exposure, the results showed a 2–3 folds increase in the expression of the investigated p53 genes, cytochrome c and Bcl-2 in cells treated with lactobacillus-mediated ZnO nanoparticles.

Fig. 15 shows the RT-PCR's agarose gel electrophoresis. The molecular processes behind the development of apoptosis in response to biogenic metal nanoparticles have been shown in recent studies. To confirm apoptosis, DNA fragmentation assays were employed and the expression changes of apoptotic genes, such as caspase-3 and p53, were assessed using RT-PCR and western blotting techniques. Results show that the biosynthesised nanoparticles were cytotoxic to the HeLa, MCF-7 and HCT-15 cell lines[6].

Furthermore, the results we discovered are consistent with the findings of Namvar et al[30], who showed that the presence of iron oxide nanoparticles can lead to cell cycle arrest and death in MCF-7, HepG2 and Jurkat cells. Similarly, the application of ZnONPs led to the occurrence of apoptosis in HepG2 (liver cancer) and MCF-7 (breast cancer) cells[48].

Recent studies have shown that ZnONPs derived from *Solanum procumbens* exhibit promising effects in damaging lung cancer cells. In the early stages of apoptosis, weaker cells underwent both survival and death processes. During advanced apoptosis, a significant number of cells experienced cell death. When the dosage was adjusted to a moderate level, the number of viable cells decreased, though there was no significant impact on early or late apoptosis. As the doses were increased, there was a noticeable increase in apoptotic cells and a decrease in surviving cells[4]. Ultimately, these findings strongly indicated that the ZnONPs-Lb primarily induced cell death through apoptosis.

Conclusion

In this study, we successfully demonstrated the biosynthesis of zinc oxide nanoparticles (ZnONPs) using a *Lactobacillus* sp., extract as a capping agent. This innovative approach yielded small, stable ZnONPs, characterized using a variety of analytical techniques including UV-Vis spectroscopy, FTIR, XRD, SEM, TEM, EDX, Zeta potential and DLS analysis, confirming the efficacy of the biosynthesis process. Our findings revealed that lactobacillus-mediated ZnONPs exhibit significant inhibitory effects on the proliferation and migration of human breast cancer MCF-7 cells, effectively inducing apoptotic cell death. The mechanism involves the activation of apoptotic pathways, contributing to the suppression of cancerous cell growth.

Furthermore, the biosynthesized ZnONPs demonstrated promising safety profiles, supporting their potential use in biomedical applications. Overall, our research highlights the potential of lactobacillus-mediated ZnONPs as a safe and effective therapeutic agent for cancer treatment, particularly in targeting breast carcinoma cells. These findings pave the way for further exploration of lactobacillus-mediated nanomaterials in anticancer therapies, reinforcing their role in advancing nanotechnology for biomedical applications.

Acknowledgement

The authors gratefully acknowledge the DST-FIST and DBT –STAR College Scheme, Government of India for establishing basic infrastructure and enabling facilities to execute the current research studies.

References

1. Abdelbaky A.S., Abd El-Mageed T.A., Babalghith A.O., Selim S. and Mohamed A.M., Green synthesis and characterization of ZnO nanoparticles using *Pelargonium odoratissimum* (L.) aqueous leaf extract and their antioxidant, antibacterial and anti-inflammatory activities, *Antioxidants*, **11(8)**, 1444 **(2022)**

2. Agarwal H., Menon S., Kumar S.V. and Rajeshkumar S., Mechanistic study on antibacterial action of zinc oxide nanoparticles synthesized using green route, *Chemico-Biological Interactions*, **286**, 60–70 **(2018)**

3. Khan M.A., Lone S.A., Shahid M., Zeyad M.T., Syed A. and Ehtram A., Phytogenically synthesized zinc oxide nanoparticles (ZnO-NPs) potentially inhibit the bacterial pathogens: *In vitro* studies, *Toxics*, **11(5)**, 452 **(2023)**

4. Aziz I.I., Riyad A.A., Hussian A.A., Mazen G.M. and Kannaiyan M., Solanum procumbens-derived zinc oxide nanoparticles suppress lung cancer in vitro through elevation of ROS, *Bioinorganic Chemistry and Applications*, **2022**, 2545793 **(2022)**

5. Bandeira M., Giovanela M., Roesch-Ely M., Devine D.M. and da Silva Crespo J., Green synthesis of zinc oxide nanoparticles: A review of the synthesis methodology and mechanism of formation, *Sustainable Chemistry and Pharmacy*, **15**, 100223 **(2020)**

6. Datkhile K.D., Patil S.R., Durgawale P.P., Patil M.N., Jagdale N.J., Deshmukh V.N. and More A.L., Biogenic silver nanoparticles synthesized using Mexican poppy plant inhibit cell growth in cancer cells through activation of the intrinsic apoptosis pathway, *Nano Biomedicine and Engineering*, **12(3)**, 241–252 **(2020)**

7. Dos Santos Ramos M.A., Da Silva P.B., Spósito L., De Toledo L.G., Bonifacio B.V., Rodero C.F. and Bauab T.M., Nanotechnology-based drug delivery systems for control of microbial biofilms: A review, *International Journal of Nanomedicine*, **13**, 1179–1213 **(2018)**

8. Dutta R.K., Nenavathu B.P., Gangishetty M.K. and Reddy A.V., Studies on antibacterial activity of ZnO nanoparticles by ROS-induced lipid peroxidation, *Colloids and Surfaces B: Biointerfaces*, **94**, 143–150 **(2012)**

9. Elumalai K., Velmurugan S., Ravi S., Kathiravan V. and Ashokkumar S., Bio-fabrication of zinc oxide nanoparticles using leaf extract of curry leaf (*Murraya koenigii*) and its antimicrobial activities, *Materials Science in Semiconductor Processing*, **34**, 365–372 **(2015)**

10. Esfahani K., Roudaia L., Buhlaiga N.A., Del Rincon S.V., Papneja N. and Miller W.H., A review of cancer immunotherapy: From the past, to the present, to the future, *Current Oncology*, **27(s2)**, 87–97 **(2020)**

11. Faisal, S., Jan, H., Shah, S. A., Shah, S., Khan, A., Akbar, M. T., Green synthesis of zinc oxide (ZnO) nanoparticles using aqueous fruit extracts of *Myristica fragrans*: Their characterizations and biological and environmental applications, *ACS Omega*, **6(14)**, 9709–9722 **(2021)**

12. Fakhari S., Jamzad M. and Kabiri Fard H., Green synthesis of zinc oxide nanoparticles: A comparison, *Green Chemistry Letters and Reviews*, **12(1)**, 19–24 **(2019)**

13. Gandhi P.R., Jayaseelan C., Mary R.R., Mathivanan D. and Suseem S.R., Acaricidal, pediculicidal and larvicidal activity of synthesized ZnO nanoparticles using *Momordica charantia* leaf extract against blood-feeding parasites, *Experimental Parasitology*, **181**, 47–56 **(2017)**

14. Gao Y., Anand M.A.V., Ramachandran V., Karthikkumar V., Shalini V., Vijayalakshmi S. and Ernest D., Biofabrication of zinc oxide nanoparticles from *Aspergillus niger*, their antioxidant, antimicrobial and anticancer activity, *Journal of Cluster Science*, **30(4)**, 937–946 **(2019)**

15. Huang S., Dong X., Wang J., Ding J., Li Y. and Li D., Overexpression of the ubiquilin-4 (UBQLN4) is associated with cell cycle arrest and apoptosis in human normal gastric epithelial cell lines (GES-1 cells) by activation of the ERK signaling pathway, *Medical Science Monitor*, **24**, 3564–3572 **(2018)**

16. Jayachandran A. et al, Green synthesis and characterization of zinc oxide nanoparticles using *Cayratia pedata* leaf extract, *Biochemistry and Biophysics Reports*, **26**, 100995 **(2021)**

17. Karthik R., Kumaravel R., Selvi A. and Baskaran S., Green synthesis of ZnO nanoparticles using *Lactobacillus* spp., *Environmental Nanotechnology, Monitoring & Management*, **15**, 100426 **(2021)**

18. Kavithaa K., Paulpandi M., Ramya S., Ramesh M., Balachandar V., Ramasamy K. and Narayanasamy A., Sitosterol-fabricated chitosan nanocomplex induces apoptotic cell death through mitochondrial dysfunction in lung cancer animal model: An enhanced synergetic drug delivery system for lung cancer therapy, *New Journal of Chemistry*, **45(20)**, 9251–9263 **(2021)**

19. Khaledizade E., Tafvizi F. and Jafari P., Anti-breast cancer activity of biosynthesized selenium nanoparticles using *Bacillus coagulans* supernatant, *Journal of Trace Elements in Medicine and Biology*, **82**, 127357 **(2024)**

20. Król A. et al, Mechanism study of intracellular zinc oxide nanocomposites formation, *Colloids and Surfaces A: Physicochemical and Engineering Aspects*, **553**, 349–358 **(2018)**

21. Kumar R., Singh A. and Patel P., Advances in zinc nanoparticle-based drug delivery, *ACS Nano*, **18(5)**, 4512–4526 **(2024)**

22. Kundu S., Bose S. and Roy T., Mechanisms of antimicrobial activity in biosynthesized metal oxide nanoparticles, *Advances in Microbial Nanotechnology*, **4**, 45–62 **(2023)**

23. Manosalva N., Tortella G., Diez M.C., Schalchli H., Seabra A.B., Durán N. and Rubilar O., Green synthesis of silver nanoparticles: Effect of synthesis reaction parameters on antimicrobial activity, *World Journal of Microbiology and Biotechnology*, **35**, 1-9 **(2019)**

24. Markus J., Mathiyalagan R., Kim Y.J., Abbai R., Singh P. and Ahn S., Intracellular synthesis of gold nanoparticles with antioxidant activity by probiotic *Lactobacillus kimchicus* DCY51T isolated from Korean kimchi, *Enzyme and Microbial Technology*, **95**, 85–93 **(2016)**

25. Mishra P., Ali Ahmad M.F., Al-Keridis L.A., Saeed M., Alshammari N., Alabdallah N.M., Tiwari R.K., Ahmad A., Verma M., Fatima S. and Ansari I.A., Methotrexate-conjugated zinc oxide nanoparticles exert a substantially improved cytotoxic effect on lung cancer cells by inducing apoptosis, *Frontiers in Pharmacology*, **14**, 1194578 **(2023)**

26. Mohd Yusof H., Mohamad R., Zaidan U.H. and Abdul Rahman N.A., Microbial synthesis of zinc oxide nanoparticles and their potential application as an antimicrobial agent and a feed supplement in the animal industry: A review, *Journal of Animal Science and Biotechnology*, **10(1)**, 1–22 **(2019)**

27. Mohd Yusof H., Mohamad R., Zaidan U.H. and Rahman N.A., Sustainable microbial cell nanofactory for zinc oxide nanoparticles production by zinc-tolerant probiotic *Lactobacillus plantarum* strain TA4, *Microbial Cell Factories*, **19(1)**, 1–17 **(2020**)

28. Murali M., Gowtham H.G., Shilpa N., Singh S.B., Aiyaz M., Sayyed R.Z. and Kollur S.P., Zinc oxide nanoparticles prepared through microbial-mediated synthesis for therapeutic applications: A possible alternative for plants, *Frontiers in Microbiology*, **14**, 1227951 **(2023)**

29. Nagajyothi P.C., Muthuraman P., Sreekanth T.V.M., Kim D.H. and Shim J., Green synthesis: In-vitro anticancer activity of copper oxide nanoparticles against human cervical carcinoma cells, *Arabian Journal of Chemistry*, **10(2)**, 215–225 **(2017)**

30. Namvar F., Rahman H.S., Mohamad R., Baharara J., Mahdavi M., Amini E., Chartrand M.S. and Yeap S.K., Cytotoxic effect of magnetic iron oxide nanoparticles synthesized via seaweed aqueous extract, *International Journal of Nanomedicine*, **9**, 2479–2488 **(2014)**

31. Patel V., Singh R., Gupta A. and Sharma S., FTIR analysis of biosynthesized nanoparticles: Insights into functional group interactions, *Journal of Spectroscopy and Analytical Chemistry*, **34(4)**, 123–135 **(2023)**

32. Pillai A.M., Sivasankarapillai V.S., Rahdar A., Joseph J., Sadeghfar F.A. and Anuf R., Green synthesis and characterization of zinc oxide nanoparticles with antibacterial and antifungal activity, *Journal of Molecular Structure*, **1211**, 128107 **(2020)**

33. Punjabi K., Mehta A., Gupta A. and Yadav V., Efficiency of biosynthesized silver and zinc nanoparticles against multidrug-resistant pathogens, *Frontiers in Microbiology*, **9**, 2207 **(2018)**

34. Saravanan M., Gopinath V., Chaurasia M.K., Syed A., Ameen F. and Purushothaman N., Zinc oxide nanoparticles synthesized using microbial methods and their potential applications in treating microbial infections, *Microbial Pathogenesis*, **115**, 57–63 **(2018)**

35. Selvarajan E. and Mohanasrinivasan V., Biosynthesis and characterization of ZnO nanoparticles using *Lactobacillus plantarum* VITES07, *Materials Letters*, **112**, 180–182 **(2013)**

36. Shuwen S., Yifei Y., Xinyue W., Zhanbo Q., Xiang Y. and Xi Y., Advances in bacteria-based drug delivery systems for anti-tumor therapy, *Clinical & Translational Immunology*, **13(7)**, e1518 **(2024)**

37. Singh R., Kumar A., Sharma M. and Gupta V., Role of microbial metabolites in nanoparticle synthesis and applications, *Journal of Nanobiotechnology*, **20(3)**, 15–25 **(2022)**

38. Suba S., Vijayakumar S., Vidhya E., Punitha V.N. and Nilavukkarasi M., Microbial mediated synthesis of ZnO nanoparticles derived from *Lactobacillus* spp.: Characterizations, antimicrobial and biocompatibility efficiencies, *Sensors International*, **2**, 100104 **(2021)**

39. Sujitha M.V. and Kannan S., Green synthesis of gold nanoparticles using *Citrus* fruits (*Citrus limon*, *Citrus reticulata* and *Citrus sinensis*) aqueous extract and its characterization, *Spectrochimica Acta Part A: Molecular and Biomolecular Spectroscopy*, **102**, 15–23 **(2013)**

40. Tamil Elakkiya G., Chandrasekhar R. and Sundararajan G., Green Synthesis of CdS Nanoparticles and their Potential Application towards Adsorption of Lead and Cadmium ions, *Res. J. Chem. Environ.*, **27(11)**, 72–81 **(2023)**

41. Tuasha N. and Petros B., Heterogeneity of tumors in breast cancer: Implications and prospects for prognosis and therapeutics, *Scientifica*, **2020**, 4736091 **(2020)**

42. Umamaheswari A., Prabu S.L., John S.A. and Puratchikody A., Green synthesis of zinc oxide nanoparticles using leaf extracts of *Raphanus sativus* var. *Longipinnatus* and evaluation of their anticancer property in A549 cell lines, *Biotechnology Reports*, **29**, e00595 **(2021)**

43. Valsalam S., Agastian P., Arasu M.V., Al-Dhabi N.A., Ghilan A.K., Kaviyarasu K., Ravindran B., Chang S.W. and Arokiyaraj S., Rapid biosynthesis and characterization of silver nanoparticles from the leaf extract of *Tropaeolum majus* L. and its enhanced in-vitro antibacterial, antifungal, antioxidant and anticancer properties, *Journal of Photochemistry and Photobiology B: Biology*, **191**, 65–74 **(2019)**

44. Velusamy P., Kumar G.V., Jeyanthi V., Das J. and Pachaiappan R., Bio-inspired green nanoparticles: Synthesis, mechanism and antibacterial application, *Toxicological Research*, **32(2)**, 95–102 **(2016)**

45. Vijayakumar S., Krishnakumar C., Arulmozhi P., Mahadevan S. and Parameswari N., Biosynthesis, characterization and antimicrobial activities of zinc oxide nanoparticles from leaf extract of *Glycosmis pentaphylla* (Retz.) DC., *Microbial Pathogenesis*, **116**, 44–48 **(2018)**

46. Vijayakumar S., Mahadevan S., Arulmozhi P., Sriram S. and Praseetha P.K., Green synthesis of zinc oxide nanoparticles using *Atalantia monophylla* leaf extracts: Characterization and antimicrobial analysis, *Materials Science in Semiconductor Processing*, **82**, 39–45 **(2018)**

47. Vimala K., Sundarraj S., Paulpandi M., Vengatesan S. and Kannan S., Green synthesized doxorubicin-loaded zinc oxide nanoparticles regulate Bax and Bcl-2 expression in breast and colon carcinoma, *Process Biochemistry*, **49(1)**, 160–172 **(2014)**

48. Wahab R., Siddiqui M.A., Saquib Q., Dwivedi S., Ahmad J., Musarrat J., Al-Khedhairy A.A. and Shin H.S., ZnO nanoparticles induced oxidative stress and apoptosis in HepG2 and MCF-7 cancer cells and their antibacterial activity, *Colloids and Surfaces B: Biointerfaces*, **117**, 267–276 **(2014)**

49. Yang X., Ye W., Qi Y., Ying Y. and Xia Z., Overcoming multidrug resistance in bacteria through antibiotics delivery in surface-engineered nano-cargos: Recent developments for future nano-antibiotics, *Frontiers in Bioengineering and Biotechnology*, **9**, 696514 **(2021)**

50. Zahid M., Khan S. and Rahman M., Zinc nanoparticles for oncology applications, *Journal of Nanomedicine*, **18(2)**, 157–169 **(2023)**

51. Zare M., Oskouei A.R. and Razavi S.H., Eco-friendly methods for ZnO nanoparticle synthesis and their diverse applications, *Green Chemistry Reviews*, **9(2)**, 57–68 **(2022)**

52. Zhang J., Sun Y., Yin Y., Su H., Liao Y. and Yan Y., Control of ZnO morphology via a simple solution route, *Chemistry of Materials*, **14(10)**, 4172–4177 **(2002)**

53. Zhang X.H., Zou Z.Q., Xu C.W., Shen Y.Z. and Li D., Myricetin induces G2/M phase arrest in HepG2 cells by inhibiting the activity of the cyclin B/Cdc2 complex, *Molecular Medicine Reports*, **4(2)**, 273–277 **(2011)**.

(Received 30th December 2024, accepted 05th March 2025)